Brain and Cognition 155 (2021) 105822

Contents lists available at ScienceDirect

Brain and Cognition

journal homepage: www.elsevier.com/locate/b&c

Morphometry and functional connectivity of auditory cortex in school-age children with profound language disabilities: Five comparative case studies

Annika Carola Linke [a,*], Dominika Slušná [b], Jiwandeep Singh Kohli [a], Juan Álvarez-Linera Prado [c], Ralph-Axel Müller [a,d], Wolfram Hinzen [b,e]

[a] Brain Development Imaging Laboratories, Department of Psychology, San Diego State University, San Diego, CA, USA
[b] Department of Translation and Language Sciences, Campus Poblenou, Pompeu Fabra University, Barcelona 08018, Barcelona, Spain
[c] Neuroradiology Department, Hospital Ruber Internacional, Madrid, Spain
[d] San Diego State University/University of California San Diego Joint Doctoral Program in Clinical Psychology, San Diego, CA, USA
[e] Institució Catalana de Recerca i Estudis Avançats, ICREA, 08010 Barcelona, Spain

ARTICLE INFO

Keywords:
Functional connectivity
Auditory language network
Neurodevelopmental disorders
Cortical morphometry
Severe language deficits

ABSTRACT

Many neurodevelopmental conditions imply absent or severely reduced language capacities at school age. Evidence from functional magnetic resonance imaging is highly limited. We selected a series of five cases scanned with the same fMRI paradigm and the aim of relating individual language profiles onto underlying patterns of functional connectivity (FC) across auditory language cortex: three with neurogenetic syndromes (Coffin-Siris, Landau-Kleffner, and Fragile-X), one with idiopathic intellectual disability, one with autism spectrum disorder (ASD). Compared to both a group with typical development (TD) and a verbal ASD group (total N = 110), they all showed interhemispheric FC below two standard deviations of the TD mean. Children with higher language scores showed higher intrahemispheric FC between Heschl's gyrus and other auditory language regions, as well as an increase of FC during language stimulation compared to rest. An increase of FC in forward vs. reversed speech in the posterior and middle temporal gyri was seen across all cases. The Coffin-Siris case, the most severe, also had the most anomalous FC patterns and showed reduced myelin content, while the Landau-Kleffner case showed reduced cortical thickness. These results suggest potential for neural markers and mechanisms of severe language processing deficits under highly heterogeneous etiological conditions.

1. Introduction

Language disorder is not confined to pathologies labeled as such (e.g., developmental language disorder or dyslexia), but is found across numerous neurodevelopmental conditions, often with severe presentations. Thus, up to 30% of children with autism spectrum disorder (ASD) are estimated to remain non- or minimally verbal throughout their lives (Slušná et al., n.d.; Tager-Flusberg & Kasari, 2013; Wodka et al., 2013). In neurogenetic syndromes such as Phelan McDermid (Wang et al., 2016), Angelman (Alvares & Downing, 1998; Margolis et al., 2015), or Coffin-Siris (Schrier et al., 2012), absence of functional language development is the rule rather than the exception, while in Landau-Kleffner syndrome (Hoshi & Miyazato, 2017; Pearl et al., 2001), language capacity regresses after three to seven years of normal language development. While children across these conditions will typically all score very low results in standardized language tests, underlying etiologies, neural mechanisms, and clinical presentations differ widely. As language plays a critical role in cognitive development and early learning (Perszyk & Waxman, 2017), illuminating these individual differences is key to develop and personalize treatments and to assess a given child's learning potential.

Even in relatively common disorders such as ASD, only a small number of studies (Lai et al., 2012; Wan et al., 2012; Jack & Pelphrey, 2017 for review) have used magnetic resonance imaging (MRI) to investigate the neural basis of failure of functional language development. Wan et al. (2012) found atypical right-lateralization in the volume of the arcuate fasciculus, a part of the dorsal language processing pathway, in four of five minimally verbal children studied. Lai et al. (2012) investigated neural responses to speech vs. musical (song) stimuli in 23 children with ASD that were classified as minimally verbal,

* Corresponding author at: Brain Development Imaging Laboratory, Department of Psychology, San Diego State University, 6363 Alvarado CT, Suite #200, San Diego, CA 92120, USA.
E-mail address: alinke@mail.sdsu.edu (A.C. Linke).

https://doi.org/10.1016/j.bandc.2021.105822
Received 7 July 2021; Received in revised form 27 October 2021; Accepted 2 November 2021
0278-2626/© 2021 The Authors. Published by Elsevier Inc. This is an open access article under the CC BY-NC-ND license (http://creativecommons.org/licenses/by-nc-nd/4.0/).

and who showed activations in left inferior frontal gyrus and secondary auditory cortex during song but not speech. In rare neurogenetic syndromes, even less is known; and in many cases, no fMRI studies at all have been performed.

The practical challenge of participant compliance when scanning children with severe difficulties of communicating verbally and intellectual disability significantly contributes to this dearth of knowledge. In the study by Lai et al. (2012), children who could not be scanned without sedation were excluded from the functional MRI analyses. A pioneering study by Wang et al. (2016) scanned eleven children with Phelan McDermid syndrome and nine comparison children with idiopathic ASD under light sedation with propofol. The former but not the latter group showed selective activity for communicative relative to non-communicative vocalizations in the right superior temporal gyrus (STG), which also correlated with better orienting toward social sounds. In line with this, several previous studies in neurotypical children have already successfully used passive listening tasks to map language-related changes in the blood-oxygen-level-dependent (BOLD) signal in infants and children under propofol sedation (Bernal et al., 2012; Gemma et al., 2016; Heinke et al., 2004; Liu et al., 2012; Souweidane et al., 1999). A replicated finding in this regard is resilience of perceptual processing of speech in primary auditory and superior temporal, but not inferior frontal cortex, under both propofol (Adapa et al., 2014; Davis et al., 2007; Gemma et al., 2016; Liu et al., 2012), and sevoflurane (Martuzzi et al., 2010). In addition, several studies of adults have found preservation under propofol sedation of functional connectivity (FC) patterns in spontaneous BOLD fluctuations in auditory and visual networks during resting state fMRI (Boveroux et al., 2010; Naci et al., 2018). The latter of these studies not only compared FC across levels of consciousness but also across two conditions, resting and auditory stimulation (story listening). Average FC increased significantly during the latter relative to resting.

Motivated by these findings, we here aimed to profile FC patterns in auditory language regions across five school-age children and adolescents with severe but highly heterogeneous language impairments. All children received MRI evaluations for medical purposes and permissions were obtained to include fMRI and DTI in their clinical imaging sessions. Inter- and intrahemispheric FC in auditory language regions were compared to normative benchmarks from two large comparisons groups, one with TD (50) and one with high-functioning ASD (N = 60). In the five cases, FC under resting and an auditory language condition (bedtime story) were compared. Moreover, the same bedtime story was both presented as normal forward and as backward speech. This was based on previous evidence that differential activation to forward vs. backward speech is even detectable in sleeping neonates (Dehaene-Lambertz et al., 2002; Peña et al., 2003; Sato et al., 2012; Vannasing et al., 2016). We reasoned that sensitivity of FC to these two specific contrasts could illuminate differential linguistic profiles in these children. Alongside functional network profiles, we also estimated structural grey matter morphometry via measures of cortical thickness, surface area and myelin content, in order to illuminate potential structural cortical correlates of differences in language disability.

2. Methods

2.1. Participants

The five individual cases of this study were selected from a special school devoted to developmental disorders affecting language. They were specifically selected for severe language delays and deviances compared to other children in this school. Individual data and test results from two standardized language tests are summarized in Table 1. Diagnoses were as follows:

Case 1: Autism spectrum disorder (ASD): A 13-year-old boy with severe difficulties both in the comprehension and use of language, though he can produce speech fluently, particularly when repeating utterances (echolalia). Radiological examination of brain structure revealed no abnormalities.

Table 1
Participant data and standardized test scores (PPVT: Peabody Picture Vocabulary Test; CEG: Test de Comprensión de Estructuras Gramaticales [test of grammatical comprehension]).

	Diagnosis	Sex (M/F)	Age at scan (years: months)	Verbal Mental Age* (PPVT-III) (years: months)	CEG* (direct punctuation)
1	ASD (Autism spectrum disorder)	M	13;4	6;10	39/48
2	ID (Intellectual Disability)	F	15;3	7;7	43/62
3	CS (Coffin-Siris syndrome)	M	8;5	3;2/3;2	31
4	LKS (Landau-Kleffner syndrome)	M	11;4	4;11/6;3	35/52
5	FX (Fragile-X syndrome)	M	5;8	3;5	19/34

*VMA and CEG evaluations were performed twice in some children, as indicated by two values in the same cell, which indicate an upwards trajectory in all children but one. The two tests were performed 5 months before the scan and five months after it, respectively. Children with single values reflect an evaluation at the earlier date.

Case 2: Current diagnosis of Idiopathic intellectual disability (ID): A 15-year-old girl with severe difficulties in expressive language as well as reading. At the time of study, she had reached a verbal mental age (VMA) of 7 years. Radiological examination of brain structure revealed no abnormalities.

Case 3: Coffin-Siris syndrome (CS): An 8-year-old boy, who shows absent speech production and severe comprehension difficulties with a VMA of 3 years. Clinical radiological examination revealed dysgenesis of the corpus callosum and a megacisterna magna consisting in an enlargement of the CSF-filled subarachnoid space in the posterior cranial fossa. CS Syndrome (Schrier et al., 2012) is a rare genetic condition caused by a mutation in any of several genes, including the ARID1A, ARID1B, SMARCA4, SMARCB1, DPF2, or SMARCE1 genes. Common symptoms include mild to severe ID, language delay, delay in motor skills, including sitting and walking, hypotonia, and difficulties in breathing, feeding, and swallowing. Hearing loss is reported in 30% to 60% of cases (Schrier et al., 2012; van der Sluijs et al., 2019).

Case 4: Landau-Kleffner syndrome (LKS): An 11-year-old boy, who faced language loss at age 6 but had recovered language capacities by the time of study, though not exceeding 6 years of VMA in receptive language. Radiological examination revealed an enlargement of the lateral ventricles, particularly on the left. LKS (Hoshi & Miyazato, 2017; Pearl et al., 2001) is an acquired epileptic aphasia with language regression in children following normal acquisition during the first three to seven years.

Case 5: Fragile-X syndrome (FX): A 5-year-old boy, who shows difficulties in structuring simple sentences, with a VMA of 3 years and production restricted to juxtaposed words and simple phrases of 2–3 elements. Radiological examination of brain structure revealed no abnormalities. FX (Willemsen & Kooy, 2017) is caused by a mutation in the FMR1 gene causing a range of developmental problems including learning disabilities and cognitive impairment. Delayed development of speech and language by age 2 is usually seen, and most males and one-third of affected females with FX have mild to moderate intellectual disability. About one-third of individuals with FX have features of ASD, affecting communication and social interaction.

3. Magnetic resonance imaging acquisitions (Madrid case series)

MRI data were collected at the Ruber International Hospital, Madrid,

on a Siemens Prisma 3 T scanner using a 64-channel head coil. The acquisition of a high-resolution T1-weighted structural image (magnetization-prepared rapid-acquisition, gradient echo sequence; TR = 2,400 msec, TE = 2.22 msec, slice thickness = 0.7999 mm, 0.8 mm in plane resolution, 208 sagittal slices, matrix size = 300 × 320) was followed by a T2-weighted structural image (TR = 3,200 msec, TE = 563 msec, slice thickness = 0.7999 mm, 208 sagittal slices, matrix size = 300 × 320). T1-weighted images for each child are shown in Fig. 1. After structural data was collected, resting state fMRI (no stimuli were presented during acquisition) was acquired. One functional run consisting of 264 (8 min 52 s) functional images sensitive to blood oxygenation level-dependent contrast (BOLD; echo planar T2*-weighted gradient echo sequence; TR = 2,000 msec, TE = 30 msec, flip angle 80°, acquisition matrix = 576 × 576, 4.37 mm in plane resolution, 3.5 mm thickness, no gap, 32 axial slices aligned to the plane intersecting the anterior and posterior commissures) was acquired. Finally, after the resting state sequence, a fMRI language task was carried out. One functional run consisted of 358 (11 min 39 s) functional images BOLD (echo planar T2*-weighted gradient echo sequence; TR = 2,000 msec, TE = 30 msec, flip angle 90°, acquisition matrix = 612 × 612, 2,35 mm in plane resolution, 3.5 mm thickness, no gap, 32 axial slices aligned to the plane intersecting the anterior and posterior commissures). The fMRI language task acquisition parameters of one participant (ASD) were different from the rest of the group: one functional run consisted of 240 (11 min 39 s) functional images BOLD (echo planar T2*-weighted gradient echo sequence; TR = 3,000 msec, TE = 30 msec, flip angle 90°, acquisition matrix = 816 × 816, 2.99 mm in plane resolution, 2.4 mm thickness, no gap, 50 axial slices aligned to the plane intersecting the anterior and posterior commissures).

4. fMRI experimental design (Madrid case series)

For the language task, we used a spontaneous narration of a short children story (*The snowman* by Raymond Briggs) recorded in child-directed speech by a female native Spanish speaker. The story was divided in 10 blocks (Forward language condition). The average block length was 20 s (range = 18.7–21.76 s). Each block contained short sentences forming a sequence of complete phrases. The ten blocks containing the original story were then recorded backward (Backward language condition).

First, the Forward language condition blocks were presented in order, with 15 s rest periods between blocks where no stimuli were presented (Rest condition). Afterwards, the Backward language condition blocks were presented in order, similarly, with 15 s rest periods in between. The off-resting periods were set to 15 s because the BOLD response in children returns to baseline levels faster than in adults (see Richter and Richter, 2003; Blasi et al. 2011).

5. Sedation procedure (Madrid case series)

Anesthesia was induced via a mask with sevoflurane. Immediately after, the intravenous line was placed and the child was transitioned to an intravenous-based anesthetic with propofol. The initial propofol dose was adjusted to render the patient motionless but able to maintain his or her airway with a laryngeal mask. Propofol dosage for induction was 1 mg/kg and after perfusion, a dosage of 8e10 mg/kg/h was administered. Dosage was decreased to 6 mg/kg/h until the end of the procedure. Both, sevoflurane and propofol have very small side effects and are drugs routinely used in pediatric neuroimaging. Duration of sedation using both drugs is very small allowing for very fast recovery times (Bernal et al., 2012). We took into account the pharmacokinetics of sevoflurane in order to ensure that functional tasks were carried exclusively under propofol anesthesia. Because of this, we induced a fast transition to propofol anesthesia after sevoflurane and also, we ran the first 18 min of the structural imaging part ensuring that the possible effect of sevoflurane in subsequent fMRI task was minimal. Indeed, the low solubility in blood of sevoflurane induces a rapidly decreasing alveolar concentration after cessation of the inhaled agent which is linked to very fast recovery times and wash out (Bernal et al., 2012; Yasuda et al., 1991).

6. Magnetic resonance imaging acquisitions (SDSU Cohort)

MRI data from typical developing (TD) children and adolescents and an age, sex and motion matched ASD group were included to compare FC patterns in the five cases. Demographic and clinical data are summarized in Table 2. Data were collected at the University of California San Diego (UCSD) Center for Functional MRI (CFMRI) on a GE 3 T

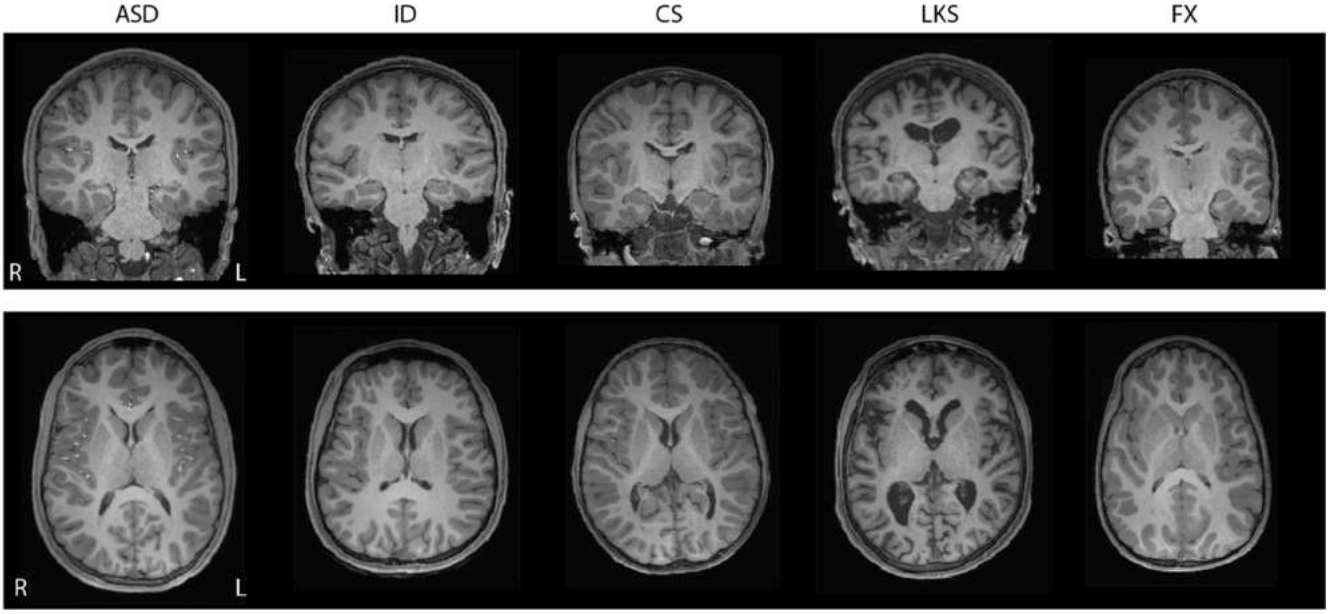

Fig. 1. T1-weighted structural images from the five cases in coronal and axial planes. Clinical radiological examination revealed no abnormalities in the ASD, ID and FX cases. In the CS case dysgenesis of the corpus callosum and a megacisterna magna consisting in an enlargement of the CSF-filled subarachnoid space in the posterior cranial fossa was detected. The LKS case showed enlargement of the lateral ventricles, particularly on the left.

Table 2
SDSU cohort.

	TD	ASD	ASD (low VIQ)	ASD vs. TD
Sample Size	50	53	7	
Age (yrs)	13.32 (2.77) [8–18]	13.76 (2.77) [7–18]	11.2 (1.2) [10–13]	t (101) = 0.82, p = .42
Sex	10F, 40 M	9F, 44 M	0F, 7 M	$\chi^2 = 0.16$, $p = .69$
Handedness	8 L, 42 R	9 L, 44 R	1 L, 6 R	$\chi^2 = 0.02$, $p = .89$
RMSD	0.06 (0.03) [0.02–0.13]	0.061 (0.03) [0.01–0.11]	0.06 (0.03) [0.2–0.098]	t (101) = 0.19, p = .85
VIQ	108 (9.7) [87–133]	103 (18.04) [59–147]	72 (6.5) [59–79]	t (101) = −1.74, p = .085
NVIQ	106 (13.36) [62–137]	106 (19.52) [53–145]	97 (17.5) [67–118]	t (98) = −0.16, p = .88
FIQ	108 (11.09) [79–132]	105 (17.31) [61–141]	83 (11.8) [61–96]	t (98) = −0.89, p = .38
SRS Total	41.8 (4.81) [35–53]	80.64 (8.91) [58–94]	83.43 (6.13) [79–94]	t (96) = 27.2, $p < .001$
ADOS Com	N/A	3.88 (1.6) [0–8]	5.86 (1.2) [4–8]	N/A
ADOS Rep	N/A	2.15 (1.35) [0–5]	1.86 (1.2) [0–4]	N/A

Discovery MR750 scanner using an 8-channel head coil. A single-shot gradient-recalled EPI sequence (180 whole-brain volumes were acquired (TR = 2000 ms; TE = 30 ms; slice thickness = 3.4 mm; flip angle = 90°; FOV = 22.0 mm; matrix = 64 × 64; in-plane resolution = 3.4 mm^2) was used to acquire 6 min of resting state fMRI. High-resolution T1-weighted sequences (3D FSPGR; 1 mm isotropic voxel size, NEX = 1, TE = min full, TI = 600, flip = 8° FOV = 25.6 cm, matrix = 256x256, receiver bandwidth 31.25htz) were collected in each participant. During all resting state functional scans, participants were presented with a white cross on a black screen and instructed to "Keep your eyes on the cross. Let your mind wander, relax, but please stay as still as you can. Try not to fall asleep." Participants' adherence to the instructions to remain awake, with eyes open, was monitored with an MR-compatible video camera. Preprocessing and FC analyses were restricted to volumes 6–170 as described below to match the number of included time points across participants.

7. MRI Preprocessing and analyses (Case series and SDSU cohort)

Structural: Cortical reconstruction and extraction of anatomical variables was performed using Freesurfer version 5.3.0-HCP (http://surfer.nmr.mgh.harvard.edu/). The processing included removal of non-brain tissue using a hybrid watershed/surface deformation procedure (Ségonne et al., 2004), automated Talairach transformation, intensity normalization (Sled et al., 1998), tessellation of the gray matter white matter boundary, automated topology correction (Fischl et al., 2001; Segonne et al., 2007), and surface deformation following intensity gradients to optimally place the gray/white and gray/cerebrospinal fluid borders at the location where the greatest shift in intensity defines the transition to the other tissue class (Dale et al., 1999; Dale & Sereno, 1993; Fischl & Dale, 2000). Further data processing and included surface inflation (Fischl, Sereno, & Dale, 1999), registration to a spherical atlas which is based on individual cortical folding patterns to match cortical geometry across subjects (Fischl, Sereno, Tootell, et al., 1999) and parcellation of the cerebral cortex into regions of interest with respect to gyral and sulcal structure (Desikan et al., 2006; Fischl et al., 2004), from which cortical thickness and surface area data were extracted. Cortical thickness, calculated as the closest distance from the gray/white boundary to the gray/CSF boundary at each vertex on the tessellated surface (Fischl & Dale, 2000). Procedures for the measurement of cortical thickness have been validated against histological analysis (Rosas et al., 2002) and manual measurements (Kuperberg et al., 2003; Salat et al., 2004) and morphometric procedures have been demonstrated to show good test–retest reliability across scanner manufacturers and across field strengths (Han et al., 2006; Reuter et al., 2012). Myelin maps were generated using the Human Connectome Project minimal processing pipelines (Glasser et al., 2013), in which cortical myelin content is estimated by dividing the T1w image by the T2w image and mapping values sampled from mid-thickness onto the cortical surface in FreeSurfer. Four bilateral regions from the Desikan atlas were included in structural analyses covering primary and secondary auditory cortices (left and right transversetemporal, superiortemporal, bankssts, and the middletemporal ROIs).

MRI data for functional connectivity (FC) analyses were preprocessed, denoised and analyzed in Matlab 2019b (Mathworks Inc., Natick, MA, USA) using SPM12 (Wellcome Trust Centre for Neuroimaging, University College London, UK), and the CONN toolbox v19b.

For the functional analysis pipeline, the structural T1-weighted image was converted from dicom to nifti format and was coregistered to the mean functional image, segmented and normalized to MNI space using non-linear registration and the default tissue probability maps included with SPM12. The white matter (WM) and cerebrospinal fluid (CSF) probability maps obtained from segmentation of the structural image for each individual subject were thresholded at 0.9 and eroded by 1 voxel and time courses extracted from the using aCompCor (Behzadi et al., 2007) for subsequent nuisance regression.

Functional: EPI images motion-corrected using rigid-body realignment and slice-timing corrected as implemented in SPM12. The Artifact Detection Toolbox (ART, as installed with conn v19b) was used to identify outliers in the functional image time series from the resulting 6 motion parameters (3 translational and 3 rotational) that had framewise displacement (FD) > 0.9 mm and/or changes in signal intensity that were greater than five standard deviations. In order to ensure that none of the findings were due to differences in apparent motion, subsequent analyses for all participants were restricted to volumes 6 to 170. This range of volumes was chosen to exclude more extensive motion at the beginning of the resting state acquisition by participant LB, motion after volume 170 during the resting state acquisition by participant CG. The same volumes were analyzed for the auditory stimulation acquisition when comparing rest and auditory stimulation FC to match duration across conditions.

Functional images were directly normalized to MNI space with the same non-linear registration as used for the structural images. Since all analyses were run on averaged voxel time series within pre-defined ROIs, no prior smoothing was applied to the data. Band-pass filtering using a temporal filter of 0.008 to 0.08 Hz was carried out as part of the nuisance regression ("simult" option in the conn toolbox) which also included scrubbing of the motion outliers detected by the ART toolbox, and regression of the 6 motion parameters and their derivatives, as well as the first five PCA component time series derived from the CSF and WM masks. The residuals of the nuisance regression were then used for all subsequent functional connectivity analyses.

8. FC analyses

Inter- and intrahemispheric FC during rest and auditory stimulation: FC estimates were derived for the rest and auditory stimulation runs separately. BOLD time series were averaged across all voxels within four bilateral auditory regions of interest (ROIs) (Heschl's gyrus (HG), planum temporale, posterior STG, posterior MTG) as defined in the Harvard-Oxford atlas. Left and right precentral gyrus were also included, as control regions in interhemispheric FC analyses. Interhemispheric FC was estimated for each bilateral ROI pair using bivariate Pearson correlation standardized with a Fisher z-transform. Intrahemispheric FC was calculated as the average FC between HG and all other ROIs in the same hemisphere. Inter- and intrahemispheric FC were

compared across participants and conditions (rest/auditory) and to the SDSU cohorts. A subgroup of SDSU ASD participants (n = 7) with low verbal IQ (VIQ < 80; 9–13 years old, all male, one left-handed) is also presented separately to aid in the interpretation of FC differences seen between the five cases and the SDSU cohort. Results for each case are shown individually rather than averaged and no statistics were carried out comparing the individual cases to the SDSU cohort due to their very distinct etiologies and clinical presentations. Differences in inter- and intrahemispheric FC magnitudes between the SDSU TD and ASD groups were tested using independent samples t-tests.

FC during forward vs. *reverse speech*: Inter- and intrahemispheric FC between the four bilateral ROIs was estimated separately for forward vs. reverse speech presentation during the auditory stimulation fMRI run and were qualitatively compared across participants. Only the two first blocks of forward and reverse speech presentation were included in analyses, in order to match available high-quality, motion-free fMRI data across participants.

9. Results

Inter- and intrahemispheric FC during rest: Interhemispheric FC of homotopic HG, pSTG, pMTG and PT was low for almost all cases and regions when compared to both the SDSU TD and ASD groups (Fig. 2, Supplementary Figure S1). Importantly, on the other hand, FC magnitude was comparable (within two standard deviations of the SDSU TD mean) for interhemispheric FC of preCG in all five children, suggesting that the lower FC magnitude observed for homotopic auditory regions was not solely due to confounding effects of site or sedation. Reductions in interhemispheric FC magnitude was most pronounced for HG and pSTG in the child with CS, and for pMTG and PT in the child with Fragile X – the two cases with the lowest VMA. The child with idiopathic ID – and the highest VMA – was the only case who showed FC magnitudes that fell within two standard deviations of the TD mean for all auditory regions. Reduced interhemispheric HG FC has previously been associated with higher ADOS Communication scores in the same SDSU ASD cohort (Linke et al. 2018; r = −0.34, p = .02; partial correlations controlling for age and RMSD; Supplementary Figure S2), suggesting that low interhemispheric FC between auditory cortical regions observed in the five cases might be related to their severe neurodevelopmental language impairment.

Intrahemispheric FC of HG to other auditory regions was comparable to that observed in the SDSU TD group only for the ASD and ID cases (with FC magnitudes falling below two standard deviations of the TD mean for the three other cases with lower VMAs, Fig. 2B). Intrahemispheric FC was also lower in the SDSU ASD group compared to the TD group ($t(1\ 0\ 1) = -1.8$, $p = .076$, Cohen's d = −0.4), and was further reduced in those with low verbal IQ ($t(55) = -2.06$, $p = .04$, Cohen's d = −0.83; Figure S1), suggesting that low intrahemispheric auditory FC might be related to neurodevelopmental language impairment. In the SDSU cohort and in the cases with CS and ASD this pattern was more prominent in the right hemisphere (i.e. lower intrahemispheric FC in the right hemisphere; Supplementary Figure S3) while the LKS case showed the opposite asymmetry pattern with substantially lower FC in the left hemisphere.

Inter- and intra-hemispheric FC during auditory stimulation: Compared to the resting state, inter- and intrahemispheric HG FC increased during auditory stimulation in the ID and LKS cases (Fig. 3A and 3B), as would be expected during passive listening as a result of bilateral auditory cortex activation even during sedation with propofol (Adapa et al., 2014; Davis et al., 2007; Frölich et al., 2017; Plourde et al., 2006). For pSTG, pMTG and PT, the magnitude of interhemispheric FC was higher during auditory stimulation for the CS case as well, while for the ASD and FX cases interhemispheric auditory FC was comparable for the two conditions or higher during the resting state scan.

Forward vs. *backward speech*: Interhemispheric FC of pSTG and pMTG was higher during forward speech presentation for all cases (except LKS for whom pSTG FC was slightly lower during forward than backward speech) while remarkably no clear patterns across cases were obvious for HG FC (Fig. 4). Thus, while the ASD and ID cases showed typical positive interhemispheric HG FC when presented with forward speech, they showed anticorrelations between bilateral HG during reverse speech. The children with LKS and FX, on the other hand, showed stronger interhemispheric HG FC during reverse speech, while strong anticorrelations were observed in the child with CS syndrome during passive listening to both forward and reverse speech.

Cortical thickness, surface area and myelin of auditory regions: Cortical thickness of auditory regions (transversetemporal, bankssts, middletemporal, superiortemporal regions as defined in the Desikan Atlas) was generally higher in the right than left hemisphere as is typically observed (Kong et al., 2018). However, cortical thickness was

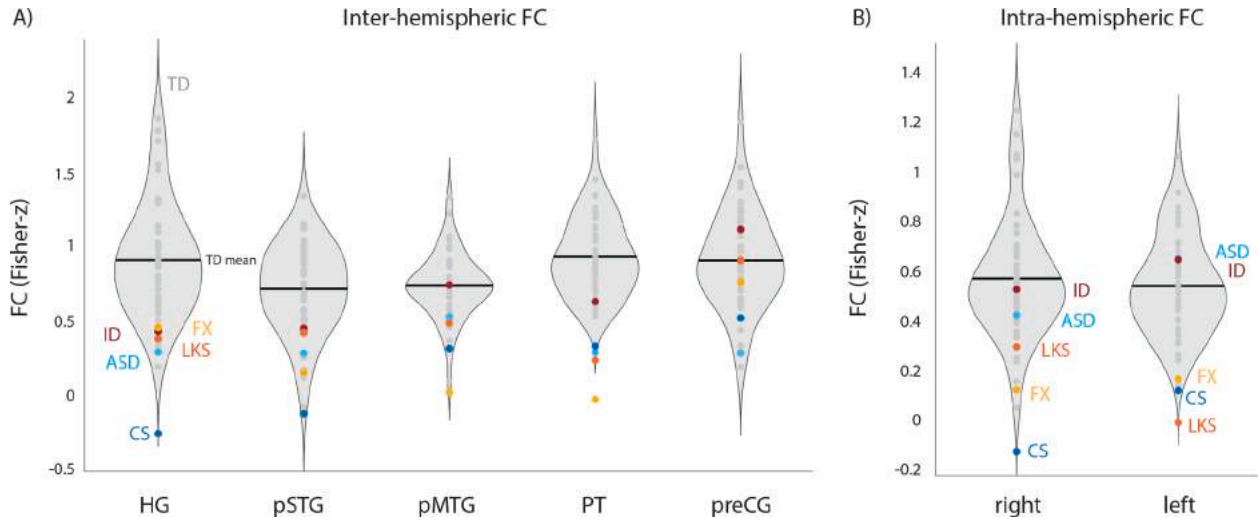

Fig. 2. A) Interhemispheric FC in auditory regions (HG, pSTG, pMTG, and PT) is reduced in the five cases with profound language impairment compared to the SDSU TD group (data shown in gray). FC in preCG fell within two standard deviations of the TD mean for all five cases suggesting that there was no global effect of reduced FC as a result of sedation (note, that interhemispheric auditory FC was not reduced as a function of deep sedation in Naci et al., 2018). B) Intrahemispheric FC (average FC of HG to other auditory regions in the same hemisphere) was two standard deviations below the TD mean for the CS case (right hemisphere) and CS and LKS case (left hemisphere) with the ASD and ID case having the most typical intrahemispheric FC. The LKS case further showed marked hemispheric differences in FC with much higher FC in the right than left hemisphere.

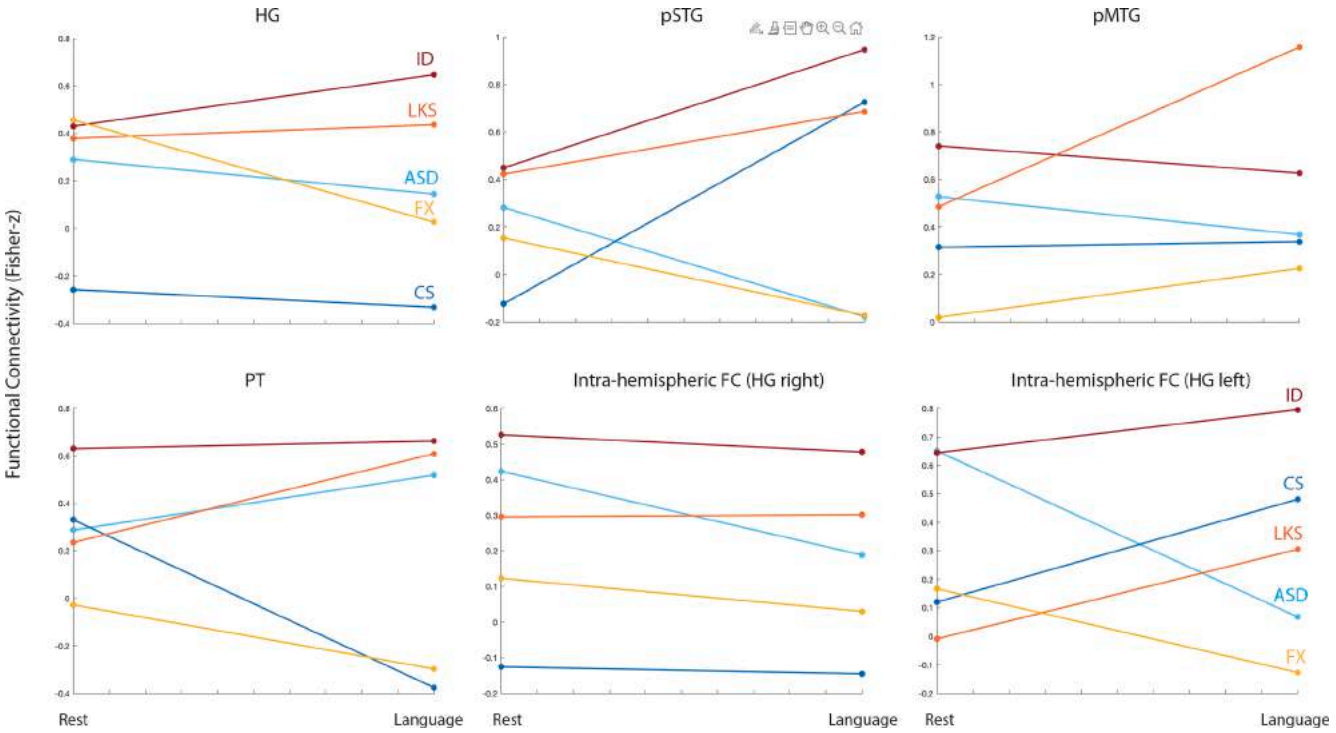

Fig. 3. FC compared between rest and auditory stimulation with spoken language in HG, pSTG, pMTG and PT for the five cases with profound language impairment. Interhemispheric FC increased during auditory language stimulation in HG, pSTG and PT in the ID and LKS case as would be expected but decreased for all regions except PT in the ASD case and except for pMTG in the FX case. The child with CS showed the most idiosyncratic pattern of interhemispheric FC changes during language stimulation across auditory regions. Intrahemispheric FC between HG and the other auditory ROIs remained similar during language stimulation compared to rest in the right hemisphere in all cases but showed an increase in FC magnitude in the left hemisphere for the ID, CS and LSK cases.

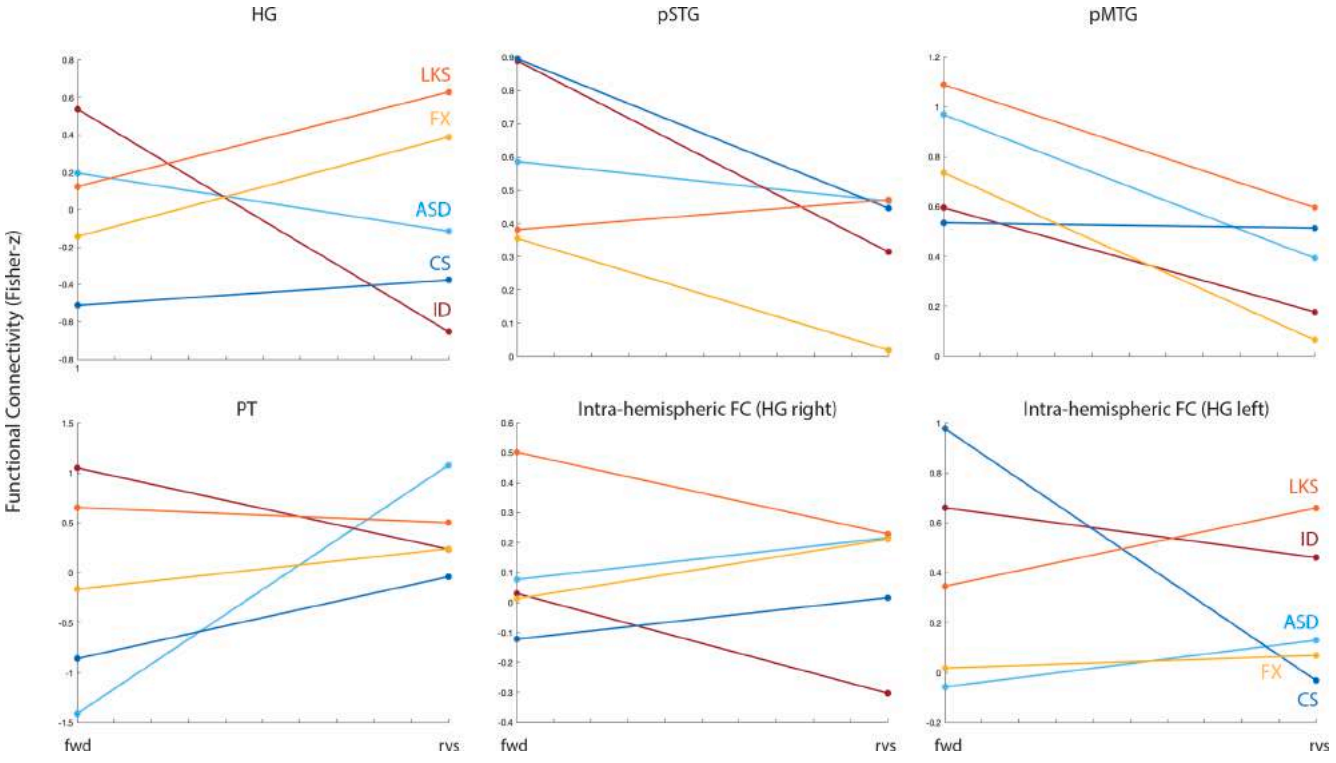

Fig. 4. FC during passive listening to forward compared to reverse speech. In pSTG and pMTG interhemispheric FC was reduced during reverse speech stimulation for all five children while changes in FC were more variable across the five cases for HG and PT, with only the child with ID showing a consistent pattern of reduced FC while listening to reverse speech for all auditory regions.

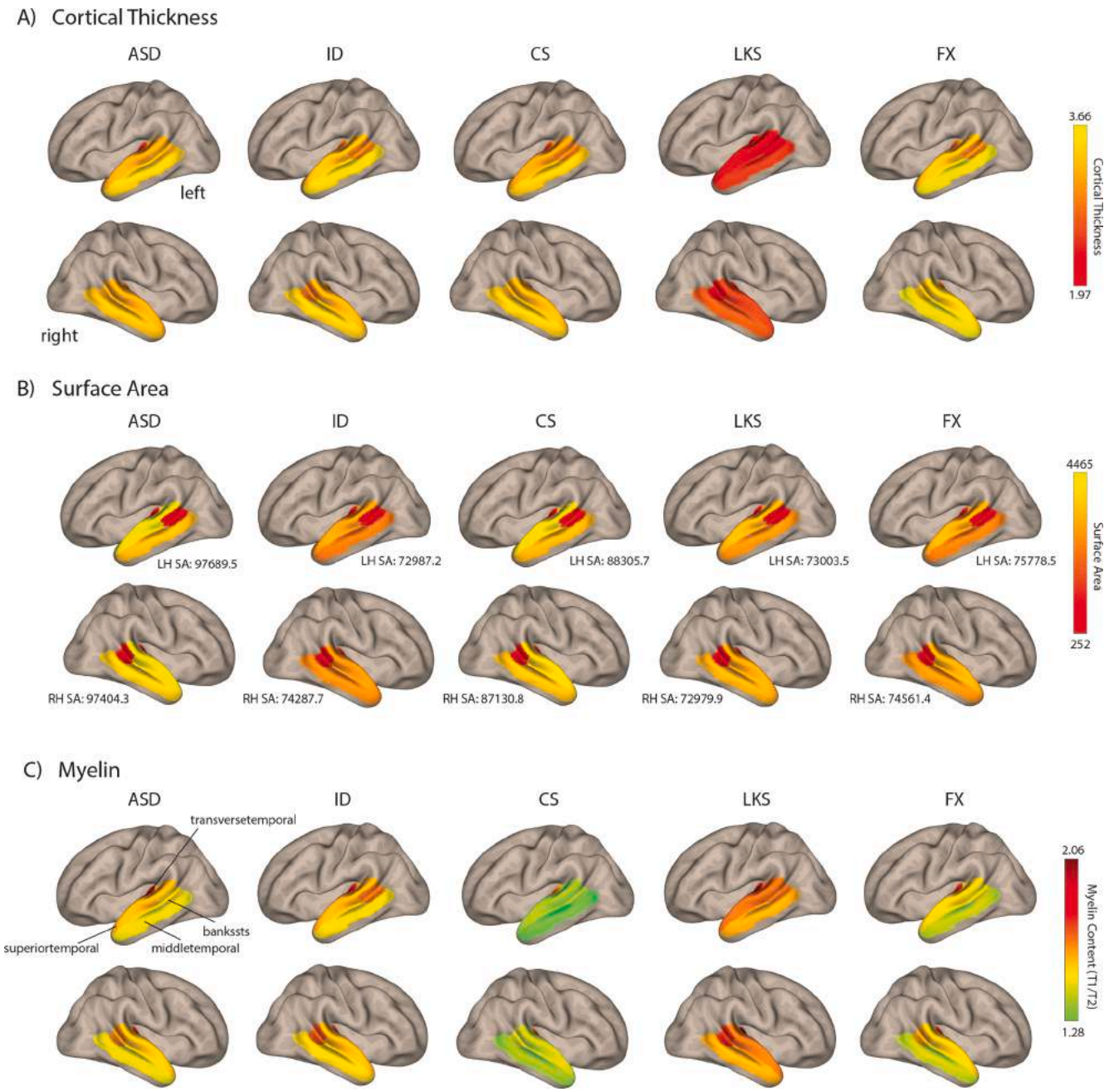

Fig. 5. A) Cortical thickness in auditory regions (using parcels from the Desikan Atlas). The LKS case shows markedly reduced cortical thickness. B) Surface Area of the same regions. Total left and right hemisphere surface areas are given as well. Surface Area increases with age but no clear age-related pattern could be observed among the 5 cases with profound language impairment. Notably, surface area was comparable across the FX (5 years, 8 months; male), ID (15 years, 3 months; female), and LKS (11 years, 4 months; male) cases with the highest overall surface areas in the ASD (13 years, 4 months; male) and CS (8 years, 5 months; male) case. C) Myelin content was calculated as the T1/T2 ratio and was substantially reduced in the child with CS.

substantially reduced in the LKS case for all four regions in both hemispheres (but more prominently in the left, Fig. 5). Surface area showed the opposite trend, with generally higher surface area in the left than right hemisphere in auditory cortical regions. Again, this follows the pattern of hemispheric asymmetries seen in the general population with primary auditory cortex (transversetemporal in the Desikan Atlas) being the region with the strongest leftward asymmetry in a study of 17,141 individuals (Kong et al., 2018). Surface Area increases with age, but no clear age-related pattern could be observed among the 5 cases with profound language impairment. Notably, surface area was comparable across the FX (5 years, 8 months; male), ID (15 years, 3 months; female), and LKS (11 years, 4 months; male) cases, with the highest overall surface areas in the ASD (13 years, 4 months; male) and CS (8 years, 5 months; male) case. Myelin content was highest in primary auditory cortex in all five cases, as would be expected (Glasser et al., 2014; Glasser & van Essen, 2011). Myelin content was markedly reduced across all auditory regions in the CS case and in all regions but primary auditory cortex (transversetemporal) in the FX case. However, it is possible that in the FX case this pattern reflects an earlier stage of maturation due to age. Myelin content was increased across all five auditory regions in the LKS case.

10. Discussion

These results reveal both a shared (or non-specific) neural index of severe language dysfunction *across* our etiologically heterogeneous cases, as well as some differentiating marks *between* them, which are meaningful in relation to their individual behavioural language scores. As for the former, low interhemispheric connectivity across all auditory language regions united all cases, while differences in intrahemispheric FC were aligned with behavioral manifestations of language impairment (VMA and CEG). Thus, the participant with ID and the highest VMA (7;7 years) and CEG scores had the highest FC values (most comparable to typical children of this age) across all regions and comparisons, while the participant with CS Syndrome and the lowest VMA (3;2) and CEG scores showed FC in the lowest range throughout, including very atypical anti-correlations in interhemispheric HG, pSTG and intrahemispheric FC on the right.

The participant with ID, moreover, showed similarities to the participant with the second-highest VMA and CEG scores (ASD), with intrahemispheric FC close to the neurotypical mean; and to the LKS case (third-highest VMA) with an expected pattern in the contrast between FC at rest and under language-stimulation (i.e. higher or unchanged FC but during language stimulation compared to resting state FC). Documented correlations between reduced inter- and intrahemispheric connectivity and social-communication and verbal IQ scores, respectively, in ASD (see Fig. S1-2), further suggest that these measures map meaningfully onto behavioral language profiles. Indeed, increased interhemispheric connectivity alongside better language outcomes have been directly linked to corpus callosum morphology, the agenesis of which, in turn, leads to connectivity disruptions related to cognitive and language impairments (Bartha-Doering et al., 2021; Hinkley et al., 2012). Corpus callosum abnormalities are a common finding not only in ASD, but also in CS Syndrome or ID (Alamri et al., 2020; Demily et al., 2019; Linke et al., 2018).

These results raise the question of why the ASD but not the LKS case showed a more surprising pattern in the rest-vs.-language contrast, with FC paradoxically *decreasing* under language stimulation compared to rest, both intrahemispherically and interhemispherically (except in the PT). We speculate that this may relate to the pathological mechanism behind language impairments in LKS and ASD. LKS is an acquired epileptic aphasia affecting auditory processing, which follows several years of normal language development, while ASD is a developmental condition, in which language is affected from its earliest manifestations (e.g. in babbling: Patten et al., 2014, or in early brain responses to language: Eyler et al., 2012; Redcay & Courchesne, 2008). Moreover, although auditory language processing anomalies in ASD are clearly prominent (O'Connor, 2012), individuals with ASD can show even greater proficiency in tasks with simple, low-level auditory stimuli (e.g., pitch discrimination: Bonnel et al., 2010). Language difficulties in ASD, however, clearly go beyond auditory perception of language, extending to deeper semantic levels and affecting comprehension and the grasp of language in its normal use to communicate thoughts in social interactions (Boucher, 2012; Hinzen et al., 2019). A history of fluent echolalia in our particular ASD case additionally reveals that auditory processing of language as such is not the issue. This may explain the above anomalous patterns of FC in the comparison of language vs. rest seen in this ASD (and the FX) case, but not the LKS case. The same applies to a similarly anomalous pattern in the comparison between forward and backward speech, where intrahemispheric FC (and interhemispheric FC in the TP) in the ASD case paradoxically *increased* for backward speech relative to forward, whereas in the ID case it decreased, in accordance with expectations.

Similar observations can be made when contrasting the ASD with the ID case. Children with ASD and ID experience marked delays as well as deviance in language development, even when compared to intellectually disabled groups matched on a test of nonverbal mental age (Bartolucci et al., 1980). Moreover, when matching ASD children to children with specific language impairment (developmental language disorder), the former did not differ from the latter in typical measures used to identify language disorder (e.g., syntactic errors), but their language development was also more severely impaired, showing signs not only of delay but also deviance (Bartak et al., 1975, 1977). Against this background it is tempting to view the above FC pattern as illustrating relative intactness of the cerebral language network in the idiopathic ID (and, less clearly, LKS) cases, while illustrating relatively more severe anomaly or deviance in the ASD case, where language is affected at a deeper level. Further in line with this speculation, *speech* in our ASD case is highly normal behaviourally (as shown by a history of highly fluent echolalia), while *language* is clearly not. The ID case may show the opposite dissociation, as speech (production and perception) is highly impaired, while there is no behavioural indication from the use of language that there is a deeper problem in grasping the essence of language or how it functions communicatively. Put differently, a problem with speech perception and production may cause an 'access' problem to language in the latter (ID) case, while language dysfunction in ASD (and FX) is likely more than that of a blocked sensory-motor access.

Continuing this line of thought, LKS as an aphasic syndrome involving an acquired loss of normal linguistic competence may be analogous to adult post-stroke aphasic syndromes, which have been described as a problem of 'access' as well. In the words of Hula & McNeil (2008: 169), the access hypothesis maintains that, in aphasia, 'language mechanisms are fundamentally preserved and that aphasic language behaviours are instead due to impairments of cognitive processes supporting their construction'. Among multiple evidence for this proposal is evidence from fMRI, which shows that functional language networks in aphasia resemble normal language control networks (Kiran et al., 2015; Ramage et al., 2020; Stefaniak et al., 2020) though in the dynamics of language recovery, right-hemisphere homologous regions may be temporarily recruited depending on the extent of left-hemisphere damage in core language regions (Saur et al., 2006). Similarly, the present study gives several indications of a right-shift in language function in the LKS case, including higher FC in the right than left hemisphere, and a more pronounced reduction of cortical thickness on the left than on the right. One previous single-case fMRI study (Datta et al., 2013) has already demonstrated that language functions in LKS can be reorganized from left to right.

Finally, LKS was also the only case to show increased grey matter myelin content alongside decreased cortical thickness across the auditory regions, in line with evidence of a relation between these two variables that has been independently established (Glasser & van Essen, 2011). Cortical myelin has been noted to impede axonal and synaptic growth (Filbin, 2003), which may obstruct cortical neuronal plasticity in areas that require higher developmental neuronal remodeling such as the lateral temporal lobe (Timmler & Simons, 2019). Reduced myelin content, on the other hand, as observed in the FX and CS cases, may give rise to abnormal generation of synaptic connections. Interestingly, CS showed the most striking pattern of inter- and intrahemispheric FC anticorrelations, while both CS and FX failed to exhibit an expected differentiation between FC during language and at rest, with striking anti-correlations seen during language in both cases.

11. Limitations

The data from our five cases were obtained under sedation, and data from the comparison groups were not. The latter moreover were obtained from a different MRI scanner and site. However, the primary focus of this study were our five cases, which we aimed to compare against each other and their associated behavioural profiles. The control groups were added as we considered it valuable to show typical FC patterns for the selected regions in a large typically developing sample as well as in children and adolescents with ASD, who often present with language impairments. Application of MRI scanning under sedation has permitted us to obtain high quality data void of confounds associated

with short acquisition times (Lai et al., 2012) or extraction of volumes with high degree of movement (Gabrielsen et al., 2018). Moreover, inside our group, high heterogeneity was seen which aligned with behavioural differences, suggesting no generic effect of sedation. In addition, when comparing FC across groups, fundamental deviations in FC were seen in auditory language processing regions, but not the precentral gyrus, which we added as a control region, again suggesting no generalized effect of sedation or scanner. As noted above, previous studies of language networks under sedation have also suggested that sensory FC patterns in temporal regions to be less affected than functional activations. Finally, we saw similar patterns across the five cases for the structural and functional data (in terms of which child showed the most atypical results), with the structural data not affected by sedation. In short, while, ideally, the data from the five cases would have been collected under the exact same conditions as those in the control groups, it would not be ethical to conduct research scans on healthy TD children under sedation.

12. Conclusions

This study has examined a collection of rare cases of severe language impairment with very different etiologies, all assessed using the same neuroimaging protocol. We conclude that FC patterns across auditory language regions along with morphometric cortical measures of these regions are promising neural markers for shedding more light on language function in children with severe language impairments, who often cannot be scanned awake. The patterns in question depict a neural diversity that meaningfully maps onto a behavioural linguistic diversity. Insights for treatments will depend on broadening the range of neurodevelopmental syndromes investigated with fMRI and similar measures, to better understand the meaning of these neural markers and create more individualized neurocognitive profiles, on which treatment and educational strategies can then be based.

13. Ethics approval

This study was approved by an institutional review board (CEIm Hospital Ruber Internacional; Sa-15842/19-EC:385), in accordance with 1964 Helsinki declaration and its later amendments. Caregivers of all participants gave their informed consent.

Declaration of Competing Interest

The authors declare that they have no known competing financial interests or personal relationships that could have appeared to influence the work reported in this paper.

Acknowledgements

We are grateful to the children and parents who contributed to this study. We also thank all teachers from the school El cole de Celia y Pepe, and specifically to Mariana Lombardo, the director of the school, for their dedication and active participation.

Funding

This research was supported by the Querer Foundation and by an 'advanced research group' grant to the Grammar and Cognition Lab [2017 SGR 1265, W.H.], and grants FFI2013-40526P and PID2019-110120RB-I00/AEI/10.13039/501100011033 by the Ministerio de Ciencia, Innovación y Universidades (MCIU) and the Agencia Estatal de Investigación (AEI) (W.H.), and a predoctoral research grant from the Generalitat de Catalunya (AGAUR) & European Social Found [2018FI_B_00860, D.S.]. The funders had no role in the study design, data collection and analysis, decision to publish, or preparation of the manuscript.

Appendix A. Supplementary material

Supplementary data to this article can be found online at https://doi.org/10.1016/j.bandc.2021.105822.

References

Adapa, R. M., Davis, M. H., Stamatakis, E. A., Absalom, A. R., & Menon, D. K. (2014). Neural correlates of successful semantic processing during propofol sedation. *Human Brain Mapping, 35*(7), 2935–2949. https://doi.org/10.1002/hbm.22375

Alamri, A., Aljadhai, Y. I., Alrashed, A., Alfheed, B., Abdelmoaty, R., Alenazi, S., Alhashim, A., & Benini, R. (2020). Identifying Clinical Clues in Children With Global Developmental Delay / Intellectual Disability With Abnormal Brain Magnetic Resonance Imaging (MRI). *Journal of Child Neurology, 36*(6), 432–439. https://doi.org/10.1177/0883073820977330

Alvares, R., & Downing, S. (1998). A survey of expressive communication skills in childen with Angelman syndrome. *American Journal of Speech-Language Pathology, 7*(2), 14–23.

Bartak, L., Rutter, M., & Cox, A. (1975). A Comparative Study of Infantile Autism and Specific Developmental Receptive Language Disorder I. *British Journal of Psychiatry, 126*(2), 127–145.

Bartak, L., Rutter, M., & Cox, A. (1977). A comparative study of infantile autism and specific developmental receptive language disorders III. Discriminant function analysis. *Journal of Autism and Childhood Schizophrenia, 7*, 383–396.

Bartha-Doering, L., Schwartz, E., Kollndorfer, K., Fischmeister, F. P. S., Novak, A., Langs, G., Werneck, H., Prayer, D., Seidl, R., & Kasprian, G. (2021). Effect of corpus callosum agenesis on the language network in children and adolescents. *Brain Structure and Function, 226*(3), 701–713. https://doi.org/10.1007/s00429-020-02203-6

Bartolucci, G., Pierce, S. J., & Streiner, D. (1980). Cross-sectional studies of grammatical morphemes in autistic and mentally retarded children. *Journal of Autism and Developmental Disorders, 10*(I), 39–50. https://doi.org/10.1007/BF02408431

Bernal, B., Grossman, S., Gonazalez, R., & Altman, N. (2012). fMRI under sedation: What is the best choice in children? *Journal of Clinical Medicine Research, 4*(6).

Behzadi, Y., Restom, K., Liau, J., & Liu, T. T. (2007). A component based noise correction method (CompCor) for BOLD and perfusion based fMRI. *NeuroImage, 37*(1), 90–101.

Bonnel, A., McAdams, S., Smith, B., Berthiaume, C., Bertone, A., Ciocca, V., Burack, J. A., & Mottron, L. (2010). Enhanced pure-tone pitch discrimination among persons with autism but not Asperger syndrome. *Neuropsychologia, 48*(9), 2465–2475. https://doi.org/10.1016/j.neuropsychologia.2010.04.020

Boucher, J. (2012). Research review: Structural language in autistic spectrum disorder - Characteristics and causes. *Journal of Child Psychology and Psychiatry and Allied Disciplines, 53*(3), 219–233. https://doi.org/10.1111/j.1469-7610.2011.02508.x

Boveroux, P., Vanhaudenhuyse, A., Bruno, M. A., Noirhomme, Q., Lauwick, S., Luxen, A., Degueldre, C., Plenevaux, A., Schnakers, C., Phillips, C., Brichant, J. F., Bonhomme, V., Maquet, P., Greicius, M. D., Laureys, S., & Boly, M. (2010). Breakdown of within- and between-network resting state functional magnetic resonance imaging connectivity during propofol-induced loss of consciousness. *Anesthesiology, 113*(5), 1038–1053. https://doi.org/10.1097/ALN.0b013e3181f697f5

Dale, A. M., Fischl, B., & Sereno, M. I. (1999). Cortical surface-based analysis I. Segmentation and surface reconstruction. *NeuroImage, 9*(2), 179–194.

Dale, A. M., & Sereno, M. I. (1993). Improved localization of cortical activity by combining EEG and MEG with MRI cortical surface reconstruction: A linear approach. *Journal of Cognitive Neuroscience, 5*, 162–176.

Datta, A. N., Oser, N., Ramelli, G. P., Gobbin, N. Z., Lantz, G., Penner, I. K., & Weber, P. (2013). BECTS evolving to Landau-Kleffner Syndrome and back by subsequent recovery: A longitudinal language reorganization case study using fMRI, source EEG, and neuropsychological testing. *Epilepsy and Behavior, 27*(1), 107–114. https://doi.org/10.1016/j.yebeh.2012.12.025

Davis, M. H., Coleman, M. R., Absalom, A. R., Rodd, J. M., Johnsrude, I. S., Matta, B. F., Owen, A. M., & Menon, D. K. (2007). Dissociating speech perception and comprehension at reduced levels of awareness. *Proceedings of the National Academy of Sciences, 104*(41), 16032–16037. https://doi.org/10.1073/pnas.0701309104

Dehaene-Lambertz, G., Dehaene, S., & Hertz-Pannier, L. (2002). Functional Neuroimaging of Speech Perception in Infants. *Science, 298*(5600), 2013–2015.

Demily, C., Duwime, C., Lopez, C., Hemimou, C., Poisson, A., Plasse, J., Robert, M. P., Dénier, C., Rossi, M., Franck, N., Besmond, C., Barcia, G., Boddaert, N., Munnich, A., & Vaivre-Douret, L. (2019). Corpus callosum metrics predict severity of visuospatial and neuromotor dysfunctions in ARID1B mutations with Coffin-Siris syndrome. *Psychiatric Genetics, 29*(6).

Desikan, R. S., Ségonne, F., Fischl, B., Quinn, B. T., Dickerson, B. C., Blacker, D., Buckner, R. L., Dale, A. M., Maguire, R. P., Hyman, B. T., Albert, M. S., & Killiany, R. J. (2006). An automated labeling system for subdividing the human cerebral cortex on MRI scans into gyral based regions of interest. *NeuroImage, 31*(3), 968–980.

Eyler, L. T., Pierce, K., & Courchesne, E. (2012). A failure of left temporal cortex to specialize for language is an early emerging and fundamental property of autism. *Brain, 135*(3), 949–960. https://doi.org/10.1093/brain/awr364

Filbin, M. T. (2003). Myelin-associated inhibitors of axonal regeneration in the adult mammalian CNS. *Nature Reviews Neuroscience, 4*(9), 703–713. https://doi.org/10.1038/nrn1195

Fischl, B., & Dale, A. M. (2000). Measuring the thickness of the human cerebral cortex from magnetic resonance images. *Proceedings of the National Academy of Sciences, 97*(20), 11050–11055.
Fischl, B., Liu, A., & Dale, A. M. (2001). Automated manifold surgery: Constructing geometrically accurate and topologically correct models of the human cerebral cortex. *IEEE Transactions on Medical Imaging, 20*(1), 70–80.
Fischl, B., Sereno, M. I., & Dale, A. M. (1999). Cortical surface-based analysis. II: Inflation, flattening, and a surface-based coordinate system. *Neuroimage, 9*(2), 195–207.
Fischl, B., Sereno, M. I., Tootell, R. B. H., & Dale, A. M. (1999). High-resolution intersubject averaging and a coordinate system for the cortical surface. *Human Brain Mapping, 8*(4), 272–284.
Fischl, B., van der Kouwe, A., Destrieux, C., Halgren, E., Segonne, F., Salat, D. H., Busa, E., Seidman, L. J., Goldstein, J., Kennedy, D., Caviness, V., Makris, N., Rosen, B., & Dale, A. M. (2004). Automatically parcellating the human cerebral cortex. *Cerebral Cortex, 14*, 11–22.
Frölich, M., Banks, A., & Ness, T. (2017). The effect of sedation on cortical activation. *Anesthesia & Analgesia, 124*(5), 1603–1610. https://doi.org/10.1213/ANE.0000000000002021.THE
Gabrielsen, T. P., Anderson, J. S., Stephenson, K. G., Beck, J., King, J. B., Kellems, R., Top, D. N., Russell, N. C. C., Anderberg, E., Lundwall, R. A., Hansen, B., & South, M. (2018). Functional MRI connectivity of children with autism and low verbal and cognitive performance. *Molecular Autism, 9*(1), 1–14. https://doi.org/10.1186/s13229-018-0248-y
Gemma, M., Scola, E., Baldoli, C., Mucchetti, M., Pontesilli, S., De Vitis, A., Falini, A., & Beretta, L. (2016). Auditory functional magnetic resonance in awake (nonsadated) and propofol-sadated children. *Pediatric Anesthesia, 26*, 521–530.
Glasser, M. F., Goyal, M. S., Preuss, T. M., Raichle, M. E., & Van Essen, D. C. (2014). Trends and properties of human cerebral cortex: Correlations with cortical myelin content. *NeuroImage, 93*, 165–175. https://doi.org/10.1016/j.neuroimage.2013.03.060
Glasser, M. F., Sotiropoulos, S. N., Wilson, J. A., Coalson, T. S., Fischl, B., Andersson, J. L., Xu, J., Jbabdi, S., Webster, M., Polimeni, J. R., Van Essen, D. C., & Jenkinson, M. (2013). The minimal preprocessing pipelines for the Human Connectome Project. *Neuroimage, 80*, 105–124.
Glasser, M. F., & van Essen, D. C. (2011). Mapping human cortical areas in vivo based on myelin content as revealed by T1- and T2-weighted MRI. *Journal of Neuroscience, 31*(32), 11597–11616. https://doi.org/10.1523/JNEUROSCI.2180-11.2011
Han, X., Jovicich, J., Salat, D., van der Kouwe, A., Quinn, B., Czanner, S., Busa, E., Pacheco, J., Albert, M., Killiany, R., Maguire, P., Rosas, D., Makris, N., Dale, A., Dickerson, B., & Fischl, B. (2006). Reliability of MRI-derived measurements of human cerebral cortical thickness: The effects of field strength, scanner upgrade and manufacturer. *NeuroImage, 32*(1), 180–194.
Heinke, W., Kenntner, R., Gunter, T. C., Sammler, D., Olthoff, D., & Koelsch, S. (2004). Sequential Effects of Increasing Propofol Sedation on Frontal and Temporal Cortices as Indexed by Auditory Event-related Potentials. *Anesthesiology, 100*(3), 617–625. https://doi.org/10.1097/00000542-200403000-00023
Hinkley, L. B. N., Marco, E. J., Findlay, A. M., Honma, S., Jeremy, R. J., Strominger, Z., Bukshpun, P., Wakahiro, M., Brown, W. S., Paul, L. K., Barkovich, A. J., Mukherjee, P., Nagarajan, S. S., Sherr, E. H., & Maurits, N. M. (2012). The role of corpus callosum development in functional connectivity and cognitive processing. *PLoS ONE, 7*(8), e39804. https://doi.org/10.1371/journal.pone.003980410.1371/journal.pone.0039804.g00110.1371/journal.pone.0039804.g00210.1371/journal.pone.0039804.g00310.1371/journal.pone.0039804.g00410.1371/journal.pone.0039804.g00510.1371/journal.pone.0039804.g00610.1371/journal.pone.0039804.g00710.1371/journal.pone.0039804.t00110.1371/journal.pone.0039804.t00210.1371/journal.pone.0039804.t00310.1371/journal.pone.0039804.t004
Hinzen, W., Slušná, D., Schroeder, K., Sevilla, G., & Vila Borrellas, E. (2019). Mind-Language = ? The significance of non-verbal autism. *Mind and Language, 34*, 1–25. https://doi.org/10.1111/mila.12257
Hoshi, K., & Miyazato, K. (2017). Architecture of Human Language from the Perspective of a Case of Childhood Architecture of Human Language from the Perspective of a Case of Childhood Aphasia — Landau – Kleffner Syndrome. *Biolinguistics, 10*(January), 136–196.
Hula, W., & McNeil, M. (2008). Models of attention and dual-task performance as explanatory constructs in aphasia. *Seminars in Speech and Language, 29*(03), 169–187.
Jack, A., & Pelphrey, A. K. (2017). Annual Research Review: Understudied populations within the autism spectrum – current trends and future directions in neuroimaging research. *Journal of Child Psychology and Psychiatry and Allied Disciplines, 58*(4), 411–435. https://doi.org/10.1111/jcpp.12687
Kiran, S., Meier, E. L., Kapse, K. J., & Glynn, P. A. (2015). Changes in task-based effective connectivity in language networks following rehabilitation in post-stroke patients with aphasia. *Frontiers in Human Neuroscience, 9*(June), 1–20. https://doi.org/10.3389/fnhum.2015.00316
Kong, X. Z., Mathias, S. R., Guadalupe, T., Abé, C., Agartz, I., Akudjedu, T. N., Aleman, A., Alhusaini, S., Allen, N. B., Ames, D., Andreassen, O. A., Vasquez, A. A., Armstrong, N. J., Bergo, F., Bastin, M. E., Batalla, A., Bauer, J., Baune, B. T., Baur-Streubel, R., … Francks, C. (2018). Mapping cortical brain asymmetry in 17,141 healthy individuals worldwide via the ENIGMA consortium. *Proceedings of the National Academy of Sciences of the United States of America, 115*(22), E5154–E5163. https://doi.org/10.1073/pnas.1718418115
Kuperberg, G. R., Broome, M. R., McGuire, P. K., David, A. S., Eddy, M., Ozawa, F., Goff, D., West, W. C., Williams, S. C., van der Kouwe, A. J., Salat, D. H., Dale, A. M., & Fischl, B. (2003). Regionally localized thinning of the cerebral cortex in schizophrenia. *Archives of General Psychiatry, 60*, 878–888.
Lai, G., Pantazatos, S. P., Schneider, H., & Hirsch, J. (2012). Neural systems for speech and song in autism. *Brain, 135*(3), 961–975. https://doi.org/10.1093/brain/awr335
Linke, A. C., Jao Keehn, R. J., Pueschel, E. B., Fishman, I., & Müller, R. A. (2018). Children with ASD show links between aberrant sound processing, social symptoms, and atypical auditory interhemispheric and thalamocortical functional connectivity. *Developmental Cognitive Neuroscience, 29*, 117–126. https://doi.org/10.1016/j.dcn.2017.01.007
Liu, X., Lauer, K. K., Ward, B. D., Rao, S. M., Li, S.-J., & Hudetz, A. G. (2012). Propofol disrupts functional interactions between sensory and high-order processing of auditory verbal memory. *Human Brain Mapping, 33*(10), 2487–2498. https://doi.org/10.1002/hbm.v33.1010.1002/hbm.21385
Margolis, S. S., Sell, G. L., Zbinden, M. A., & Bird, L. M. (2015). Angelman Syndrome. *Neurotherapeutics, 12*(3), 641–650. https://doi.org/10.1007/s13311-015-0361-y
Martuzzi, R., Ramani, R., Qiu, M., Rajeevan, N., & Constable, R. T. (2010). Functional connectivity and alterations in baseline brain state in humans. *NeuroImage, 49*(1), 823–834. https://doi.org/10.1016/j.neuroimage.2009.07.028
Naci, L., Haugg, A., MacDonald, A., Anello, M., Houldin, E., Naqshbandi, S., Gonzalez-Lara, L. E., Arango, M., Harle, C., Cusack, R., & Owen, A. M. (2018). Functional diversity of brain networks supports consciousness and verbal intelligence. *Scientific Reports, 8*(1). https://doi.org/10.1038/s41598-018-31525-z
O'Connor, K. (2012). Auditory processing in autism spectrum disorder: A review. *Neuroscience and Biobehavioral Reviews, 36*(2), 836–854. https://doi.org/10.1016/j.neubiorev.2011.11.008
Pearl, P. L., Carrazana, E. J., & Holmes, G. L. (2001). The Landau-Kleffner Syndrome. *Epilepsy Currents, 1*(2), 39–45.
Peña, M., Maki, A., Kovačić, D., Dehaene-Lambertz, G., Koizumit, H., Bouquet, F., & Mehler, J. (2003). Sounds and silence: An optical topography study of language recognition at birth. *Proceedings of the National Academy of Sciences of the United States of America, 100*(20), 11702–11705. https://doi.org/10.1073/pnas.1934290100
Perszyk, D. R., & Waxman, S. R. (2017). Linking Language and Cognition in Infancy. *Annual Review of Psychology*, 1–20. https://doi.org/10.1146/annurev-psych-122216-011701
Plourde, G., Belin, P., Chartrand, D., Fiset, P., Backman, S. B., Xie, G., & Zatorre, R. J. (2006). Cortical processing of complex auditory stimuli during alterations of consciousness with the general anesthetic propofol. *Anesthesiology, 104*(3), 448–457. https://doi.org/10.1097/00000542-200603000-00011
Ramage, A. E., Aytur, S., & Ballard, K. J. (2020). Resting-state functional magnetic resonance imaging connectivity between semantic and phonological regions of interest may inform language targets in aphasia. *Journal of Speech, Language and Hearing Research, 63*(9), 3051–3067.
Redcay, E., & Courchesne, E. (2008). Deviant Functional Magnetic Resonance Imaging Patterns of Brain Activity to Speech in 2–3-Year-Old Children with Autism Spectrum Disorder. *Biological Psychiatry, 64*(7), 589–598. https://doi.org/10.1016/j.biopsych.2008.05.020
Reuter, M., Schmansky, N. J., Rosas, H. D., & Fischl, B. (2012). Within-subject template estimation for unbiased longitudinal image analysis. *NeuroImage, 61*(4), 1402–1418.
Rosas, H. D., Liu, A. K., Hersch, S., Glessner, M., Ferrante, R. J., Salat, D. H., van der Kouwe, A., Jenkins, B. G., Dale, A. M., & Fischl, B. (2002). Regional and progressive thinning of the cortical ribbon in Huntington's disease. *Neurology, 58*, 695–701.
Salat, D. H., Buckner, R. L., Snyder, A. Z., Greve, D. N., Desikan, R. S., Busa, E., Morris, J. C., Dale, A. M., & Fischl, B. (2004). Thinning of the cerebral cortex in aging. *Cerebral Cortex, 14*, 721–730.
Sato, H., Hirabayashi, Y., Tsubokura, H., Kanai, M., Ashida, T., Konishi, I., Uchida-Ota, M., Konishi, Y., & Maki, A. (2012). Cerebral hemodynamics in newborn infants exposed to speech sounds: A whole-head optical topography study. *Human Brain Mapping, 33*(9), 2092–2103. https://doi.org/10.1002/hbm.v33.910.1002/hbm.21350
Saur, D., Lange, R., Baumgaertner, A., Schraknepper, V., Willmes, K., Rijntjes, M., & Weiller, C. (2006). Dynamics of language reorganization after stroke. *Brain, 129*(6), 1371–1384. https://doi.org/10.1093/brain/awl090
Schrier, S. A., Bodurtha, J. N., Burton, B., Chudley, A. E., Chiong, M. A. D., Davanzo, M. G., Lynch, S. A., Musio, A., Nyazov, D. M., Sanchez-Lara, P. A., Shalev, S. A., & Deardorff, M. A. (2012). The Coffin-Siris syndrome: A proposed diagnostic approach and assessment of 15 overlapping cases. *American Journal of Medical Genetics, Part A, 158A*(8), 1865–1876. https://doi.org/10.1002/ajmg.a.35415
Ségonne, F., Dale, A. M., Busa, E., Glessner, M., Salat, D., Hahn, H. K., & Fischl, B. (2004). A hybrid approach to the skull stripping problem in MRI. *Neuroimage, 22*(3), 1060–1075.
Segonne, F., Pacheco, J., & Fischl, B. (2007). Geometrically accurate topology-correction of cortical surfaces using nonseparating loops. *IEEE Transactions on Medical Imaging, 26*(4), 518–529.
Sled, J. G., Zijdenbos, A. P., & Evans, A. C. (1998). A nonparametric method for automatic correction of intensity nonuniformity in MRI data. *IEEE Transactions on Medical Imaging, 17*(1), 87–97.
Slušná, D., Rodríguez, A., Salvadó, B., Vicente, A., & Hinzen, W. (n.d.). *Relations between language, non-verbal cognition and conceptualization in non- or minimally verbal individuals with ASD across the lifespan*.
Souweidane, M. M., Kim, K. H., McDowall, R., Ruge, M. I., Lis, E., Krol, G., & Hirsch, J. (1999). Brain mapping in sedated infants and young children with passive-functional magnetic resonance imaging. *Pediatric Neurosurgery, 30*(2), 86–92. DOI: pne30086 [pii].

Stefaniak, J. D., Halai, A. D., & Lambon Ralph, M. A. (2020). The neural and neurocomputational bases of recovery from post-stroke aphasia. *Nature Reviews Neurology, 16*(1), 43–55. https://doi.org/10.1038/s41582-019-0282-1

Tager-Flusberg, H., & Kasari, C. (2013). Minimally verbal school-aged children with autism spectrum disorder: The neglected end of the spectrum. *Autism Research, 6*(6), 320–331. https://doi.org/10.1002/nbm.3066.Non-invasive

Timmler, S., & Simons, M. (2019). Grey matter myelination. *Glia, 67*(11), 2063–2070.

van der Sluijs, P. J., Jansen, S., Vergano, S. A., Adachi-Fukuda, M., Alanay, Y., AlKindy, A., Baban, A., Bayat, A., Beck-Wödl, S., Berry, K., Bijlsma, E. K., Bok, L. A., Brouwer, A. F. J., van der Burgt, I., Campeau, P. M., Canham, N., Chrzanowska, K., Chu, Y. W. Y., Chung, B. H. Y., … Santen, G. W. E. (2019). The ARID1B spectrum in 143 patients: from nonsyndromic intellectual disability to Coffin-Siris syndrome. *Genetics in Medicine, 21*(6), 1295–1307. https://doi.org/10.1038/s41436-018-0330-z

Vannasing, P., Florea, O., González-Frankenberger, B., Tremblay, J., Paquette, N., Safi, D., Wallois, F., Lepore, F., Béland, R., Lassonde, M., & Gallagher, A. (2016). Distinct hemispheric specializations for native and non-native languages in one-day-old newborns identified by fNIRS. *Neuropsychologia, 84*, 63–69. https://doi.org/10.1016/j.neuropsychologia.2016.01.038

Wan, C. Y., Marchina, S., Norton, A., & Schlaug, G. (2012). Atypical hemispheric asymmetry in the arcuate fasciculus of completely nonverbal children with autism. *Annals of the New York Academy of Sciences, 1252*, 332–337. https://doi.org/10.1111/j.1749-6632.2012.06446.x.Atypical

Wang, A. T., Lim, T., Jamison, J., Bush, L., Soorya, L. V., Tavassoli, T., Siper, P. M., Buxbaum, J. D., & Kolevzon, A. (2016). Neural selectivity for communicative auditory signals in Phelan-McDermid syndrome. *Journal of Neurodevelopmental Disorders, 8*(1), 1–11. https://doi.org/10.1186/s11689-016-9138-9

Willemsen, R., & Kooy, F. R. (2017). *Fragile X Syndrome: From Genetics to Targeted Treatment*. Academic Press.

Wodka, E. L., Mathy, P., & Kalb, L. (2013). Predictors of phrase and fluent speech in children with autism and severe language delay. *Pediatrics, 131*(4), e1128–e1134. https://doi.org/10.1542/peds.2012-2221

Yasuda, N., Lockhart, S. H., Eger, E. I., Weiskopf, R. B., Liu, J., Laster, M., Taheri, S., & Peterson, N. A. (1991). Comparison of kinetics of sevoflurane and isoflurane in humans. *Anesthesia & Analgesia, 72*(3), 316–324.